

Toy models of crossed Andreev reflection

R. Mélin^{*(1)}, H. Jirari⁽¹⁾ and S. Peysson⁽²⁾

⁽¹⁾*Centre de Recherches sur les Très Basses Températures (CRTBT)[†]
CNRS BP 166X, 38042 Grenoble Cedex, France*

⁽²⁾*Instituut voor Theoretische Fysica, Universiteit van Amsterdam,
Valckenierstraat 65, 1018XE Amsterdam, The Netherlands*

(December 2, 2024)

We propose toy models of crossed Andreev reflection in multiterminal hybrid structures containing out-of-equilibrium conductors. We apply the description to two possible experiments: (i) to a device containing a large quantum dot inserted in a crossed Andreev reflection circuit. (ii) To a device containing an Aharonov-Bohm loop inserted in a crossed Andreev reflection circuit.

PACS numbers: 74.80.Fp, 72.10.Bg

I. INTRODUCTION

Transport of correlated pairs of electrons in solid state devices has focussed an important interest recently. Because of the progress in the fabrication of nanoscopic devices it will be possible to realize in a near future transport experiments in which two normal metal or spin polarized electrodes are connected to a superconductor within a distance smaller than the BCS coherence length. Transport theory of multiterminal hybrid structures has been investigated recently with various methods (a scattering approach in Ref. [1], lowest order perturbation in Ref. [2], Keldysh formalism in Ref. [3]). Multiterminal hybrid structures can be used to manipulate entangled pairs of electrons in solid state devices [1–8] and propose new tests of quantum mechanics with electrons such as EPR [4,5,8] or quantum teleportation experiments [7]. It has been suggested recently [9] that proximity effect experiments at a ferromagnet / superconductor interface could be explained by spatially separated Cooper pairs in which the spin-up (spin-down) electron propagates in a spin-up (spin-down) domain. This gives a strong motivation for investigating new situations involving spatially separated pairs of electrons, which we do in this article. One of the possible experiments that we propose involves a large quantum dot inserted in a crossed Andreev reflection circuit. This device can be used to probe spin accumulation related to crossed Andreev reflection and elastic cotunneling. Another device that we propose involves an Aharonov-Bohm loop inserted in a crossed Andreev reflection circuit. This device can be used to probe Aharonov-Bohm oscillations associated to spatially separated pairs of electrons.

The theoretical description is based on toy models relying on a series of simplifying assumptions. The initial electrical circuit is replaced by nodes interconnected by tunnel matrix elements [10]. Each node corresponds to

a large quantum dot so that the energy levels form a continuum within each node. We suppose that the propagators within a given node are uniform in space. A ferromagnetic node is thus characterized the spin-up and spin-down density of state. A superconducting node is characterized by the ordinary and anomalous propagators. We suppose that the applied voltages are small compared to the superconducting gap and that the propagators at a given node are independent on energy. Each node is supposed to be in local equilibrium so that the distribution function within each node is represented by the Fermi-Dirac distribution. To impose Kirchoff laws we determine the spin-up and spin-down chemical potentials so that the spin-up and spin-down currents are conserved at each node [10].

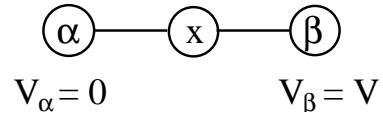


FIG. 1. The toy model used to discuss the interplay between elastic cotunneling and sequential tunneling. The local chemical potential at node x is determined in such a way that current is conserved.

II. M/M/M JUNCTION

Let us first consider the metal / metal / metal junction on Fig. 1 in which we suppose that a large quantum dot (node x) is inserted in between two metallic electrodes represented by nodes α and β . We first calculate the Green's functions $G_{i,j}$ of the connected system that are the solution of the chain of Dyson equations given by $G = g + g \otimes \Sigma \otimes G$ in a compact notation [11], where Σ is the self energy that contains all couplings of the tunnel

*melin@polycnrs-gre.fr

[†]U.P.R. 5001 du CNRS, Laboratoire conventionné avec l'Université Joseph Fourier

Hamiltonian given by

$$\mathcal{W} = t_{\alpha,x}c_{\alpha}^{\dagger}c_x + t_{x,\alpha}c_x^{\dagger}c_{\alpha} + t_{\beta,x}c_{\beta}^{\dagger}c_x + t_{x,\beta}c_x^{\dagger}c_{\beta}.$$

The symbol \otimes includes a convolution over time arguments and a summation over the labels of the network. Since there is no magnetic flux one has $t_{\alpha,x} = t_{x,\alpha}$ and $t_{x,\beta} = t_{\beta,x}$. To obtain the current flowing from node α to node x we evaluate the Keldysh Green's functions given by $G^{+,-} = (1 + G^R \otimes \Sigma) \otimes g^{+,-} \otimes (1 + \Sigma \otimes G^A)$ [11,12]. The current is related to the Keldysh Green's function by the relation [11]

$$I_{\alpha,x} = \frac{e^2}{h} \int [t_{\alpha,x}G_{\alpha,x}^{+,-}(\omega) - t_{x,\alpha}G_{\alpha,x}^{+,-}(\omega)] d\omega. \quad (1)$$

The chemical potential μ_x in the intermediate region is deduced from the Kirchoff law $I_{\alpha,x} = I_{x,\beta}$:

$$\mu_x = \frac{t_{\alpha,x}^2 \rho_{\alpha} \mu_{\alpha} + t_{\beta,x}^2 \rho_{\beta} \mu_{\beta}}{t_{\alpha,x}^2 \rho_{\alpha} + t_{\beta,x}^2 \rho_{\beta}}. \quad (2)$$

As expected if $t_{\alpha,x} = t_{\beta,x}$ and if $\rho_{\alpha} = \rho_{\beta}$ we obtain $\mu_x = \frac{1}{2}(\mu_{\alpha} + \mu_{\beta})$. The value of the conductance is easily deduced from Eq. (2):

$$G = \frac{e^2}{h} \frac{4\pi^4 t_{\alpha,x}^2 t_{\beta,x}^2 \rho_{\alpha} \rho_{\beta} \rho_x^2}{\mathcal{D}^2} \quad (3)$$

$$\times \left[1 + \frac{1}{\pi^2 t_{\alpha,x}^2 \rho_{\alpha} \rho_x + \pi^2 t_{\beta,x}^2 \rho_{\beta} \rho_x} \right], \quad (4)$$

with $\mathcal{D} = 1 + \pi^2 t_{\alpha,x}^2 \rho_{\alpha} \rho_x + \pi^2 t_{\beta,x}^2 \rho_{\beta} \rho_x$. We recognize a contribution due to elastic cotunneling and a contribution due to sequential tunneling.

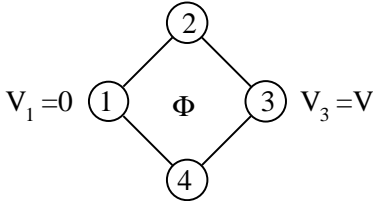


FIG. 2. The toy model used to discuss Aharonov-Bohm oscillations. A voltage $V_1 = 0$ is applied on node 1 and a voltage $V_3 = V$ is applied on node 3. The chemical potentials at nodes 2 and 4 are determined in such a way that current is conserved.

III. AHARONOV-BOHM OSCILLATIONS IN NORMAL STRUCTURES

To discuss Aharonov-Bohm oscillations we consider the toy model on Fig. 2. We consider a symmetric structure in which $\rho = \rho_1 = \rho_3$ and $\rho' = \rho_2 = \rho_4$, and we use the notation $x = \pi^2 t^2 \rho \rho'$. The conductance is given by

$$G = \frac{e^2}{h} \frac{4x}{1 + 4x + 2x^2(1 - \cos \Phi)} \quad (5)$$

which oscillates with the applied magnetic flux. As a consequence our toy model can be used to describe Aharonov-Bohm oscillations.

IV. CROSSED ANDREEV REFLECTION

Now we discuss crossed Andreev reflection [1–3]. We consider the same toy model as on Fig. 1 but now node x is superconducting. We denote by ρ_{α}^{\uparrow} , $\rho_{\alpha}^{\downarrow}$, ρ_{β}^{\uparrow} and $\rho_{\beta}^{\downarrow}$ the density of states of spin-up and spin-down electrons in electrodes α and β . We note g the ordinary propagator of the superconducting node and f the anomalous propagator. We show that f and g should satisfy the relation $f^2 = g^2$. Solving the Dyson equation and evaluating the Dyson-Keldysh equation leads to the transport formula

$$I_{\alpha,x}^{\uparrow} = -\frac{2e^2}{h} V_{\alpha} \frac{4\pi^2 t_{x,\alpha}^2}{\mathcal{D}^A \mathcal{D}^R} f^2 \rho_{\alpha}^{\uparrow} \rho_{\alpha}^{\downarrow} \quad (6)$$

$$- \frac{e^2}{h} (V_{\alpha} - V_{\beta}) \frac{4\pi^2 t_{x,\alpha}^2 t_{x,\beta}^2}{\mathcal{D}^A \mathcal{D}^R} |g^{\downarrow}|^2 \rho_{\alpha}^{\uparrow} \rho_{\beta}^{\uparrow} \quad (7)$$

$$- \frac{e^2}{h} (V_{\alpha} + V_{\beta}) \frac{4\pi^2 t_{x,\alpha}^2 t_{x,\beta}^2}{\mathcal{D}^A \mathcal{D}^R} f^2 \rho_{\alpha}^{\uparrow} \rho_{\beta}^{\downarrow}, \quad (8)$$

where the determinant \mathcal{D} is given by $\mathcal{D}^A = 1 - i\pi g(\Gamma^{\uparrow} + \Gamma^{\downarrow}) + \pi^2(f^2 - g^2)\Gamma^{\uparrow}\Gamma^{\downarrow}$, and where $\Gamma^{\uparrow} = |t_{x,\alpha}|^2 \rho_{\alpha}^{\uparrow} + |t_{x,\beta}|^2 \rho_{\beta}^{\uparrow}$ and $\Gamma^{\downarrow} = |t_{x,\alpha}|^2 \rho_{\alpha}^{\downarrow} + |t_{x,\beta}|^2 \rho_{\beta}^{\downarrow}$. The function g^{\downarrow} is given by $g^{\downarrow} = g + i\pi(f^2 - g^2)\Gamma^{\downarrow}$. The term (6) corresponds to local Andreev reflections, the term (7) corresponds to elastic cotunneling and the term (8) corresponds to crossed Andreev reflection. In microscopic models it is possible to show that because of averaging between the different conduction channels the conductance associated to crossed Andreev reflection is equal to the conductance associated to elastic cotunneling [2,3]. This cannot be demonstrated in our toy model because we lost all information about the spatial dependence of the propagators in the superconductor. Instead we choose the propagators f and g in such a way that the conductance associated to elastic cotunneling is identical to the conductance associated to crossed Andreev reflection. This leads to the condition $f^2 = g^2$. This condition ensures the equality of the Andreev reflection and elastic cotunneling currents also for large interface transparencies.

V. EFFECT OF AN OUT-OF-EQUILIBRIUM CONDUCTOR

Now we discuss a device containing a large quantum dot inserted in a crossed Andreev reflection circuit. The geometry of the device is shown on Fig. 3 and the toy model is shown on Fig. 4. Without the quantum dot the current response is symmetric: for the toy model on Fig. 1 with node x being superconducting the

crossed conductance $\mathcal{G}_{\alpha,\beta} = \partial I_{\alpha}(V_{\alpha}, V_{\beta}) / \partial V_{\beta}$ is equal to $\mathcal{G}_{\beta,\alpha} = \partial I_{\beta}(V_{\beta}, V_{\alpha}) / \partial V_{\alpha}$ [2,3]. As it is visible on Fig. 5 such symmetry relations are not valid for the device on Fig. 3. Some limiting cases can be understood on simple grounds. For $x = 0$ node 1 is a half-metal spin-up ferromagnet and nodes 2 and 3 are half-metal spin-down ferromagnets.

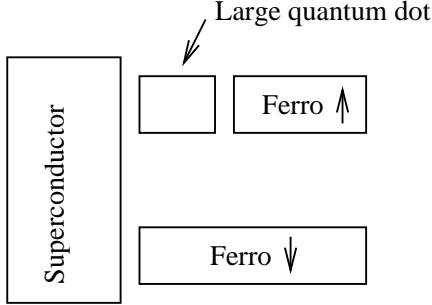


FIG. 3. Geometry of the device in which a large quantum dot is inserted in a crossed Andreev reflection circuit.

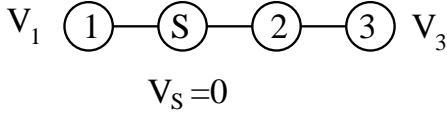


FIG. 4. The toy model corresponding to Fig. 3. Node 1 corresponds to the spin-down electrode on Fig. 3. Node 3 corresponds to the spin-up electrode and node 2 corresponds to the large quantum dot.

If we suppose that $V_1 = V \neq 0$ and $V_3 = V_S = 0$ we see that there is no voltage difference between the superconductor and node 3. As a consequence the spin-down electrons arising from crossed Andreev reflection cannot be transmitted to node 3 and there is no current, in agreement with Fig. 5. If we suppose that $V_1 = 0$, $V_3 = V \neq 0$ and $V_S = 0$ we see that spin-down electrons arising from crossed Andreev reflection can be transmitted to node 3 because there is a voltage difference between the superconductor and node 3. There is a finite current, in agreement with Fig. 5.

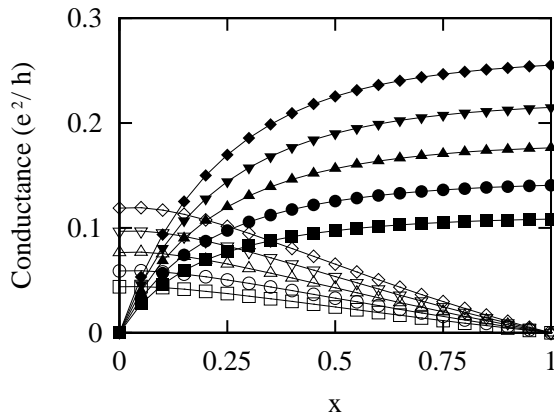


FIG. 5. Comparison between the crossed conductances in two situations for the toy model on Fig. 4: (i) $V_1 = 0$ and $V_3 = V$ (open symbols); and (ii) $V_1 = V$ and $V_3 = 0$ (filled symbols). The density of states are given by $\rho_N = 1$, $\rho_{1,\uparrow} = 1$, $\rho_{1,\downarrow} = 0$, $\rho_{2,\uparrow} = x$, $\rho_{2,\downarrow} = 1$, $\rho_{3,\uparrow} = x$ and $\rho_{3,\downarrow} = 1$. The different curves correspond to different values of the hopping parameter: $t = 0.11$ (\square and \blacksquare); $t = 0.12$ (\circ and \bullet); $t = 0.13$ (\triangle and \blacktriangle); $t = 0.14$ (∇ and \blacktriangledown); $t = 0.15$ (\diamond and \blacklozenge).

For $x = 1$ node 1 is a half-metal spin-up ferromagnet, nodes 2 and 3 are normal metal. The toy model predicts that the crossed conductance is finite if $V_1 = V \neq 0$, $V_3 = 0$ and is zero if $V_1 = 0$ and $V_3 = V \neq 0$. The case $V_1 = 0$ and $V_3 = V \neq 0$ can be understood from a cancellation between the currents due to crossed Andreev reflection and elastic cotunneling. The case $V_1 = V \neq 0$, $V_3 = 0$ is more complex because it involves spin accumulation at node 2 in the presence of elastic cotunneling and crossed Andreev reflection. Spin-up electrons from node 2 are transferred to node 1 because of elastic cotunneling. Because of crossed Andreev reflection spin-up electrons are transferred to node 1 and spin-down electrons are transferred to node 2. The rate of the two processes is identical and a naive argument would suggest that the spin-up and spin-down chemical potentials at node 2 take opposite values and that no charge current is flowing from node 2 to node 3 but only a spin current is flowing. As seen on Fig. 5 this is not the case since we find a finite charge current flowing from node 2 to node 3. We suggest that the naive reasoning does not work because the distribution function at node 2 may be affected by the fact that the two electrons arising from crossed Andreev reflection have an opposite energy whereas elastic cotunneling is at constant energy. This may induce a non trivial distribution function at node 2.

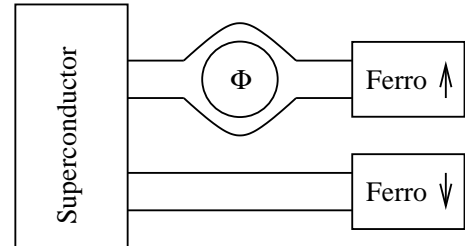


FIG. 6. Geometry of the Aharonov-Bohm experiment.

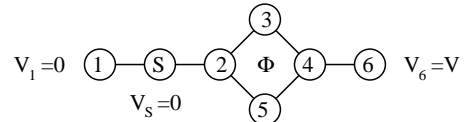


FIG. 7. The toy model used to discuss the Aharonov-Bohm experiment represented on Fig. 6.

VI. AHARONOV-BOHM EFFECT RELATED TO PAIR STATES

Now we consider the device on Fig. 6 in which an Aharonov-Bohm loop is inserted in a crossed Andreev reflection circuit and we use the toy model on Fig. 7. We first consider that the Aharonov-Bohm loop is a half-metal ferromagnet. In this case the only phenomenon coming into account is crossed Andreev reflection for antiparallel spin orientations and elastic cotunneling for parallel spin orientations. We obtain Aharonov-Bohm oscillations with a negative magnetoresistance (see Fig. 8). It may be difficult to probe this situations in experiments because the phase coherence length in ferromagnetic metals is very small. This is why we consider the case where the Aharonov-Bohm loop is made of a normal metal. Several phenomena come into account: (i) crossed Andreev reflection; (ii) elastic cotunneling; (iii) spin accumulation in the Aharonov-Bohm loop (the local spin-up and spin-down chemical potentials are not equal); (iv) electroflux effect similar to Ref. [13] (the local chemical potential oscillates with the magnetic flux applied on the Aharonov-Bohm loop). Another possible process occurring in this structure with highly transparent interfaces is that the two electrons of a Cooper pair are transferred into the Aharonov-Bohm loop, couple to the magnetic flux and come back in the other electrode. As it is visible on Fig. 9 we obtain also Aharonov-Bohm oscillations but with a positive magnetoresistance.

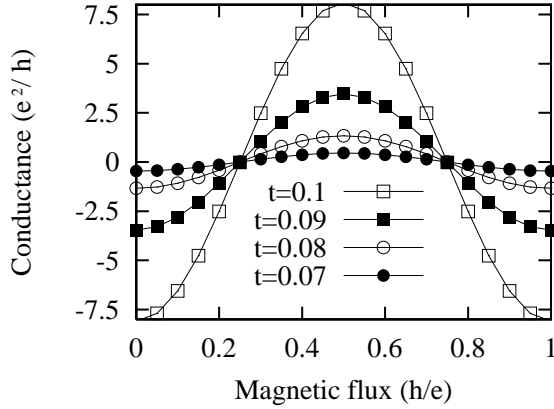


FIG. 8. Aharonov-Bohm effect related to non separable correlations. Node 1 is a half-metal spin-up ferromagnet and the Aharonov-Bohm loop is a half-metal spin-down ferromagnet: $\rho_{i,\uparrow} = 1$ and $\rho_{i,\downarrow} = 0$, $i = 2, \dots, 6$. We have shown the variation of $G_{S,1}(\Phi) - G_{S,1}^{\text{av}}$ as a function of Φ . The average conductance defined as $G_{S,1}^{\text{av}} = (G_{S,1}(\Phi = 0) + G_{S,1}(\Phi = \pi))/2$ is positive. The tunnel amplitudes are identical for all links of the network: $t = 0.1$ (\square); $t = 0.09$ (\blacksquare); $t = 0.08$ (\circ); $t = 0.07$ (\bullet). We obtain the same oscillations with a parallel spin orientation of the ferromagnetic electrodes but with an opposite current.

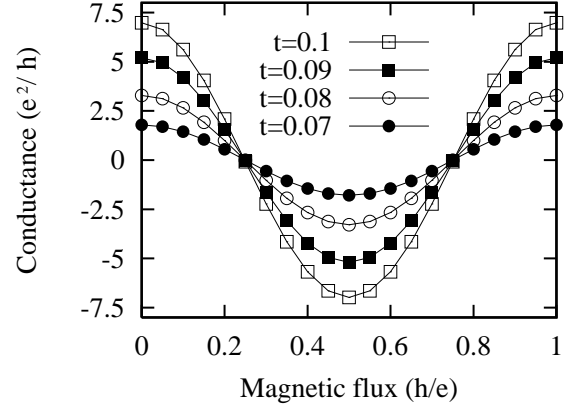


FIG. 9. The same as Fig. 8 but now nodes 2, ..., 5 are unpolarized: $\rho_{i,\uparrow} = \rho_{i,\downarrow} = 1$ with $i = 2, \dots, 5$.

VII. CONCLUSION

To summarize we have provided a toy model of multiterminal hybrid structures containing large quantum dots. We applied the model to a device in which a large quantum dot is inserted in a crossed Andreev reflection circuit. We also proposed another possible experiment intended to probe an Aharonov-Bohm effect related to spatially separated pairs of electrons. These two situations may be the object of future experiments. The description was based on a toy model in which the initial electrical circuit is replaced by a set of nodes interconnected by tunnel matrix elements. It is expected that the qualitative behavior is captured by our toy model. The formulation of a microscopic theory is left as an important open question. Within a microscopic theory it would be possible to discuss rigorously the role played by the elastic mean free path and the phase coherence length. In our toy model each node is described by a single propagator. As a consequence we have lost all information about the spatial variation of the propagators and we suppose implicitly that the distance between the contacts is smaller than the elastic mean free path. But qualitatively for the device on Fig. 6 the current is proportional to the square of the anomalous propagator in the superconductor, and to the square of the ordinary propagator in the normal metal electrodes. We have supposed in our toy model that the distance D between the contacts on the superconductor is much smaller than the BCS coherence length ξ_{BCS} and the length R of the normal metal electrodes is much smaller than the phase coherence length l_ϕ . Qualitatively the conductances on Figs. 5, 8 and Fig. 9 should thus be multiplied by the exponential factors $\exp(-D/\xi_{\text{BCS}})$ and $\exp(-R/l_\phi)$. Another important ingredient is the role played by interface transparencies. We could solve the toy model with arbitrary interface transparencies and obtained in some cases a crossed conductance larger than e^2/h with large interface transparencies. As discussed previously the value

of the conductance would be much smaller in a microscopic model because of the exponential dependence of the propagators in the superconductor. To gain in realism it would be also interesting to discuss diffusive models in connection with the occurrence of h/e oscillations in the conductance predicted from the toy model. h/e oscillations have been also obtained for the proximity effect in other geometries (see Ref. [14]).

The authors acknowledge fruitful discussions with D. Feinberg.

-
- [1] G. Deutscher and D. Feinberg, App. Phys. Lett. **76**, 487 (2000).
 - [2] G. Falci, D. Feinberg, and F.W.J. Hekking, Europhysics Letters **54**, 255 (2001).
 - [3] R. Mélin and D. Feinberg, Eur. Phys. J. B **26**, 101 (2002).
 - [4] G.B. Lesovik, T. Martin, and G. Blatter, Eur. Phys. J. B **24**, 287 (2001).
 - [5] M. S. Choi, C. Bruder and D. Loss, Phys. Rev. B **62**, 13569 (2000);
P. Recher, E. V. Sukhorukov and D. Loss, Phys. Rev. B **63**, 165314 (2001).
P. Recher and D. Loss, preprint cond-mat/0205484.
D.S. Saraga and D. Loss, preprint cond-mat/0205553.
 - [6] R. Mélin, J. Phys.: Condens. Matter **13**, 6445 (2001);
 - [7] O. Sauret, D. Feinberg and T. Martin, preprint cond-mat/0203215.
 - [8] V. Bouchiat, N. Chtchelkatchev, D. Feinberg, G.B. Lesovik, T. Martin and J. Torrès, preprint cond-mat/0206005.
 - [9] M. Giroud, K. Hasselbach, H. Courtois, D. Mailly and B. Pannetier, preprint cond-mat/0204140.
 - [10] Y. V. Nazarov, Phys. Rev. Lett. **73**, 1420 (1994);
Y.V. Nazarov, Superlattices Microst. **25**, 1221 (1999).
 - [11] C. Caroli, R. Combescot, P. Nozières and D. Saint-James, J. Phys. C **4**, 916 (1971); *ibid.* **5**, 21 (1972).
 - [12] J.C, Cuevas, A. Martin-Rodero, A. Levy Yeyati, Phys. Rev. B **54**, 736 (1996).
 - [13] T.H. Stoof and Y.V. Nazarov, Phys. Rev. B **54**, R772 (1996).
 - [14] H. Yoshioka and H. Fukuyama, Physica C **185-189**, 1625.